Vol. 74: 231–250, 2018
https://doi.org/10.3354/cr01503

CLIMATE RESEARCH
Clim Res

Published online February 15

Extreme precipitation and drought monitoring in northeastern China using general circulation models and pan evaporation-based drought indices

Muhammad Abrar Faiz[1], Dong Liu[1,2,*], Qiang Fu[1], Dariusz Wrzesiński[3], Faisal Baig[4], Ghulam Nabi[5], Muhammad Imran Khan[1], Tianxiao Li[1], Song Cui[1]

[1]School of Water Conservancy & Civil Engineering, [2]Key Laboratory of Effective Utilization of Agricultural Water Resources of Ministry of Agriculture, and Heilongjiang Provincial Collaborative Innovation Center of Grain Production Capacity Improvement, and Key Laboratory of Water-Saving Agriculture, Ordinary University in Heilongjiang Province, Northeast Agricultural University, Harbin, Heilongjiang 150030, PR China

[3]Adam Mickiewicz University, Department of Hydrology and Water Management, Poznań, Poland

[4]Department of Civil Engineering, Middle East Technical University, Ankara, Turkey

[5]Centre of Excellence in Water Resources Engineering, University of Engineering & Technology, Lahore, Pakistan

ABSTRACT: The evaluation of precipitation extremes and the usage of appropriate drought indices are very important for assessment of natural disasters (i.e. floods and drought). For this purpose, we calculated values of indices that reflect precipitation extremes and 3 drought indices, i.e. the composite index (CI), standardized precipitation evapotranspiration index (SPEI), and reconnaissance drought index (RDI), with reformulation of pan evaporation and Penman–Monteith equations (denoted as CI-Pan, RDI-Pan, RDI-PM, and SPEI-PM), based on observed data fom 1961–2005. Output from Coupled Model Intercomparison Project Phase 5 (CMIP5) historical model simulations was also used to identify discrepancies in the model simulations. The results showed that wet-day precipitation increased at a rate of 1.9 mm yr^{-1} over the entire study area. During the whole time period, the simple daily intensity index exhibited a non-significant decreasing trend compared to other precipitation indices. The number of consecutive wet days showed a negative trend, while the number of consecutive dry days showed a positive trend with a slope of 0.33 d yr^{-1}. Very small differences were found between the results of the multi-model ensemble mean and the values of the extreme precipitation indices assessed from the *in situ* stations. The performance of reformulated drought indices is significant in monitoring drought events in the study area. A comparison of the indices showed that the performance of reformulated drought indices is better than that of the standard RDI and SPEI at all stations. The highest CI-Pan value (0.23) was observed in July, and the 2 lowest values, −0.6 and −0.7, were observed in April and September, respectively, indicating that the latter 2 months are highly prone to drought.

KEY WORDS: Drought · Precipitation · General circulation model · Water resources management · Pan Evaporation

1. INTRODUCTION

During the late 20th century, extreme precipitation events are thought to have increased in the mid- and high-latitude areas of the Northern Hemisphere, and these increases are projected to continue in the 21st century (Alexander et al. 2006, IPCC 2013, Cohen et al. 2014, Trenberth et al. 2014). These precipitation extremes aggravate the intensity, frequency, and duration of disasters, such as floods and droughts

*Corresponding author: liudong5511@sina.com

(You et al. 2008, Marengo et al. 2009). In recent years, climatic precipitation extremes have received worldwide attention because of their increasing influence on agriculture and human life (Goswami et al. 2006, Boccolari & Malmusi 2013, Fu et al. 2013, Zhang et al. 2013). Assessment of these events depends on high-quality hydrometeorological variables, such as stream flow, precipitation, and temperature. Wet and dry spells can occur due to day-to-day variability in precipitation (Klein Tank & Können 2003, Ratan & Venugopal 2013). Precipitation simulation analyses using regional climate models (RCMs) or general circulation models (GCMs) can reconstruct the climatology. Analysis or assessment of the characteristics of near-future wet or dry spells based on RCMs or GCMs relative to a baseline period is of great significance (Beniston et al. 2007, May 2008). However, these results need to be validated against historical observations (such as precipitation data).

In China, several studies have been carried out using observational data to document the spatial and temporal trends and behavior of extreme precipitation at national and regional scales that show increases and decreases relative to the baseline period (Yang & Lau 2004, Qian et al. 2007, You et al. 2008, Liu et al. 2013, Wang et al. 2013). For example, Zhai et al. (1999) used observational data to identify a statistically significant increasing trend in rainy days. Wang et al. (2008) used historical records from 1961–2010 and found a slight change in the annual extreme precipitation over the Dongjiang River Basin in southern China. Li et al. (2010) and Guo et al. (2013) studied the behavior of extreme precipitation in southern China and found an increase and decrease in extreme precipitation indices in the northern and southern parts of China, respectively, whereas decreasing trends were noted in the central Tibetan Plateau. Results from Qian et al. (2007) showed that the frequency and intensity of extreme precipitation events have significantly increased in eastern China, but decreased in northern China.

Moreover, in recent years, scientists have also used different techniques and climatic models to assess spatial and temporal patterns of precipitation extremes. For example, Zhang et al. (2006) used scenario B2 from the Intergovernmental Panel on Climate Change for the periods 1961–1990 and 2070–2100, and determined the frequency of extreme precipitation events that would occur over China. Xu et al. (2005) used Providing Regional Climates for Impact Studies (PRECIS) to study changes in extreme precipitation under scenarios A2 and B2 for the period 2071–2100 and predicted that precipitation will increase over China. Li et al. (2013) used 13 Coupled Model Intercomparison Project Phase 5 (CMIP5) models, and assessed how closely the CMIP5 models resembled observations to investigate future climate extremes.

The Songhua River Basin (SRB) is located in the mid-high latitudes of northeastern China. In recent years, natural hazards, such as floods and droughts, have occurred in the SRB. For example in 1998 and 2013, summer rainstorms occurred, and 2001 and 2003 were years of prolonged drought in the region. The investigation of extreme precipitation events is very important to address natural hazards in the basin. Several publications have reported variations in precipitation in northeastern China (Table 1). Furthermore, validation of extreme precipitation events based on GCMs using observations is very important for ensuring the future safety of the water system, but the assessment of extreme precipitation based on GCMs is complex because these GCMs have large biases, due to their coarse resolution

Table 1. Key results of studies conducted in northeastern China to examine and assess variations in precipitation

Study	Time period	Results
Khan et al. (2016)	1961–2013	Monthly precipitation showed significant increasing trends during the winter season
F. Li et al. (2014)	1960–2009	Annual precipitation greatly fluctuated; a decadal decline has occurred since the 1980s
Fu et al. (2013)	1961–2009	Monthly distribution of extreme precipitation events is more unevenly distributed than monthly precipitation
Zhang et al. (2011)	1960–2000	Decrease in annual precipitation in Northeast China
Liang et al. (2011)	1961–2008	Precipitation decrease occurred at 77 (annual) and 80 (summer) of 98 meteorological stations over a 48 yr period
Qian & Lin (2005)	1961–2000	A warm-wet climate state was found in the northern part of northeast China
Zhai & Pan (2003)	1950–2000	Extreme intense precipitation events clearly increased in much of northwestern China, but decreased in the eastern part of northeastern China and most parts of North China

Table 2. Definitions of the indices used to characterize extreme precipitation. RR: daily precipitation

Index	Name	Definition	Units
RDI	Reconnaissance Drought Index	Reconnaissance Drought Index on 3-month scale	–
CI	Composite index	Composite drought index on a monthly scale	–
SPEI	Standardized Precipitation Evapotranspiration Index	Standardized Precipitation Evapotranspiration Index on 3-month scale	–
PM	Penman–Monteith	FAO-56 Penman–Monteith equation for reference evapotranspiration calculation	mm d^{-1}
Pan	Pan Evaporation	In-situ station based Pan Evaporation values for reformulation of drought indices	mm d^{-1}
CDD	Consecutive dry days	Maximum number of consecutive days with daily precipitation <1 mm	d
SDII	Simple daily intensity index	Annual total precipitation divided by the number of wet days (daily precipitation >1 mm) in the year	mm d^{-1}
PRCPTOT	Wet-day precipitation	Annual total precipitation based on wet days	mm
RX1day	Maximum 1 d precipitation	Annual maximum 1 d precipitation	mm
R99	Extreme very-wet day	Annual total precipitation when RR >N99th percentile of the daily precipitation	mm
R20mm	Number of very heavy precipitation days	Annual count of days when RR ≥20 mm	d
CWD	Consecutive wet days	Maximum number of consecutive wet days	d

(Willems et al. 2012). Mehran et al. (2014) analyzed the accuracy and bias of total precipitation in CMIP5 historical simulations as part of the Global Precipitation Climatology Project. The results showed that the overall patterns of precipitation displayed by the observations and the multi-model ensemble mean are in good agreement over most parts of the globe, but some regions showed large discrepancies.

We investigated how large the discrepancies in historical CMIP5 models are, and what spatiotemporal changes in extreme precipitation events have occurred in the SRB. To investigate this, indices to characterize extreme precipitation (Table 2) and GCMs (Table 3) were selected to assess the variations in extreme precipitation events and discrepancies in historical GCM simulations.

Assessment of evapotranspiration by accurate methods is a significant contribution towards water resources management. Distinctions are made between the concept of reference evapotranspiration and potential evapotranspiration. Reference evapotranspiration is the evapotranspiration rate from a reference crop (grass), under adequate water supply, while potential evapotranspiration is the amount of water transpired from a short green crop with uniform height and sufficient water in the soil profile. The Penman–Monteith equation is a robust method to estimate reference evapotranspiration of

Table 3. Details of historical outputs from the CMIP5 general circulation models for the period 1961–2005

GCM	Model	Source	Spatial resolution (Lon. × Lat.)
1	BCC-CSM 1.1(m)	Beijing Climate Center, China Meteorological Administration, China	1.125° × 1.125°
2	BNU-ESM	Beijing Normal University, China	2.812° × 2.812°
3	CanESM2	Canadian Centre for Climate Modelling and Analysis, Canada	2.812° × 2.812°
4	GFDL-CM3	Geophysical Fluid Dynamics Laboratory, USA	2.5° × 2°
5	CCSM4	National Center for Atmospheric Research (NCAR), USA	1.25°× 1.25°
6	GISS-E2-H	NASA Goddard Institute for Space Studies, USA	2.5° × 2°
7	IPSL-CM5A-LR	Institute Pierre-Simon Laplace, France	3.75° × 1.875°
8	MIROC-ESM	AORI, NIES, JAMSTEC, Japan	2.812° × 2.812°
9	MPI-ESM-LR	Max Planck Institute for Meteorology, Germany	1.875° × 1.875°
10	FGOALS-g2	Institute of Atmospheric Physics, Chinese Academy of Sciences, China	2.812° × 3.0°
11	CSIRO-Mk3.6.0	Australian Commonwealth Scientific and Industrial Research Organization, Australia	1.875° × 1.875°

a reference crop (grass), which considers the physical processes involved in evapotranspiration (Allen et al. 1989). Some studies used the Hargreaves & Samani (1985) (HS) equation, to estimate evapotranspiration, and compared it with other methods. Generally, the HS method is used due to its simplicity. Ravazzani et al. (2012) concluded that the HS method over- and underestimated evapotranspiration at different elevations of alpine river basins compared to the Food and Agriculture Organization 56 Penman–Monteith (FAO-56 PM) method. Other researchers evaluated the performance of the HS method in different climatic regions and documented that in humid regions, HS overestimated potential evapotranspiration and thus ranked last among methods used in the study of humid regions (Trajkovic & Kolakovic 2009, Martinez & Thepadia 2010, Ren et al. 2016). Bochetti et al. (2016) compared daily evapotranspiration obtained from HS, Priestley-Taylor and FAO-56 PM with evapotranspiration estimated by the pan evaporation method and concluded that HS underestimated evapotranspiration values. Christiansen (1968) developed a method based on pan evaporation to measure evapotranspiration and concluded that this method could accurately estimate evapotranspiration at monthly time steps. In hydrological models, an assumption has been made that there is a complementary relationship between pan evaporation and actual evaporation (Bouchet 1963, Yue et al. 2003). Some researchers concluded that a decrease in pan evaporation rate reflects a decrease in actual evaporation (Peterson et al. 1995, Brutsaert & Parlange 1998). Pan evaporation is an evaporative water loss from a standardized pan. The difference between observed and expected trends of pan evaporation is called the evaporation paradox (Roderick & Farquhar 2002). Decreases in pan evaporation or reference evapotranspiration rates may primarily be caused by aerosol concentration, decreased sunlight due to increased cloud coverage, reduction of wind speed due to monsoon change, and decreased vapor pressure deficit due to increasing air humidity (Peterson et al. 1995, Chattopadhyay & Hulme 1997, Stanhill & Cohen 2001, Cohen et al. 2002, Roderick & Farquhar 2002). Many studies have also been conducted in China to assess the variation in reference evapotranspiration and pan evaporation. The results suggested that the evaporation paradox exists in China, as decreasing rates of reference evapotranspiration and pan evaporation were observed together with an increasing trend in temperature (Liu et al. 2004, Ren & Guo 2006, Wu et al. 2006, Cong et al. 2009).

In addition, a number of drought indices have also been developed considering different methods of evapotranspiration and water balance equations. The drought indices used potential evaporation, soil moisture, rainfall, ground water or surface water (Zargar et al. 2011, Hao & AghaKouchak 2013). For example, the standardized precipitation evapotranspiration index (SPEI) incorporates water balance and evapotranspiration (Vicente-Serrano et al. 2010). The Palmer drought severity index (PDSI) considers precipitation, temperature, soil moisture, and evapotranspiration (Palmer 1965). The PDSI could be used with basic data such as long records of temperature and precipitation. The composite index (CI), developed by the National Climate Center of China, is based on precipitation and evapotranspiration (Liu et al. 2009, Qian et al. 2011), and the reconnaissance drought index (RDI) calculates the aggregated deficit between precipitation and evaporative demand of the atmosphere (Tsakiris & Vangelis 2005, Tsakiris et al. 2007). In the literature, these well-known indices are extensively used in many regions of the world, but unfortunately researchers have not been able to conclude whether certain indices are better than others due to limitations of methods used and complexity of drought (Zargar et al. 2011, Tigkas et al. 2012, Waseem et al. 2015). For instance, SPEI could be sensitive when potential evapotranspiration is calculated based on the Thornthwaite equation, since simplified forms of calculating potential evapotranspiration may produce biases in estimates (Vicente-Serrano et al. 2010). This overestimation in estimates is verified by recent studies (Sheffield et al. 2012, B. Li et al. 2014). Furthermore, PDSI is limited by soil moisture conditions as well as the effects of factors such as spatial variability of soil, catchment hydrological process, topography, and vegetation cover (Yan et al. 2013). The CI can estimate droughts at different time scales, which allows a comparison of drought events at different stations (Liu et al. 2009). Moreover, the CI also has some drawbacks in the areas where formation of spring drought is related to soil water storage of the previous autumn, and to spring precipitation before the soil thaws (Shen et al. 1980).

Multi-scalar drought indices such as RDI or SPEI are able to characterize different types of drought (Vicente-Serrano et al. 2010). The RDI has been tested in many parts of the world and performs well at commercial and regional levels. In its original formulation, RDI incorporates maximum and minimum temperatures as part of the evapotranspiration calculation, and can be used for drought monitoring and assessment (Zargar et al. 2011, Banimahd & Khalili

2013, Vangelis et al. 2013). In addition to the above, the CI, RDI, and SPEI have different theoretical backgrounds; for example, CI estimates drought through a combination of evapotranspiration evaluated by the FAO-56 PM equation and precipitation, whereas the RDI and SPEI estimate drought based on temperature data methods such as Hargreaves, Thornthwaite and Blaney-Criddle. However, for the calculation of evapotranspiration, the FAO-56 PM requires additional inputs, such as wind speed, air temperature (minimum and maximum), net radiation (Mj m^{-2} d^{-1}), and relative humidity. Considering the above scenario regarding the limitations of complete sets of climate data for the FAO-56 PM and soil moisture estimations based only on temperature, these methods may not be able to fully describe climate variability. Therefore, we reformulated the CI, RDI and SPEI indices to use pan evaporation, reference evapotranspiration, and precipitation. Moreover, the RDI and SPEI indices were also calculated with the FAO-56 PM equation to make a robust comparison among indices. In this article, the original drought indices are denoted by CI, RDI, and SPEI while the indices after modification by pan evaporation and the FAO-56 PM are denoted CI-Pan, RDI-Pan, RDI-PM, and SPEI-PM. These indices were assessed in the SRB for the period 1961–2005.

Considering the aforementioned context, the aims of this study were (1) to examine the recent trends of precipitation extremes in the SRB; (2) to assess the discrepancies in historical CMIP5 model simulations with respect to precipitation extremes; (3) to monitor the drought events based on standard (CI, RDI, and SPEI) and reformulated drought indices; (4) to make a robust comparison among indices; and (5) to provide an alternative drought index by assessing pan evaporation instead of complete sets of climatic data.

2. STUDY AREA AND DATA SETS

2.1. Study area

The SRB, located in the northeastern part of China, is the seventh largest major river basin of China with an area of 556 800 km^2. The main stream of the Songhua River includes several subcatchments, which span a range of longitudes (125° 00′–130° 98′ E) and latitudes (42° 78′–49° 30′ N; Fig. 1). The total annual precipitation ranges from 461 to 640 mm, and the mean annual air temperature ranges from 1 to 5°C. The region experiences rainy summers and cold winters (Khan et al. 2016, Liu et al. 2016, Faiz et al. 2017). The main crops are corn, soybean, and sorghum in the river catchments. Natural hazards (droughts and floods) frequently occur in the river catchments. Careful management of the 939 km long river catchment is

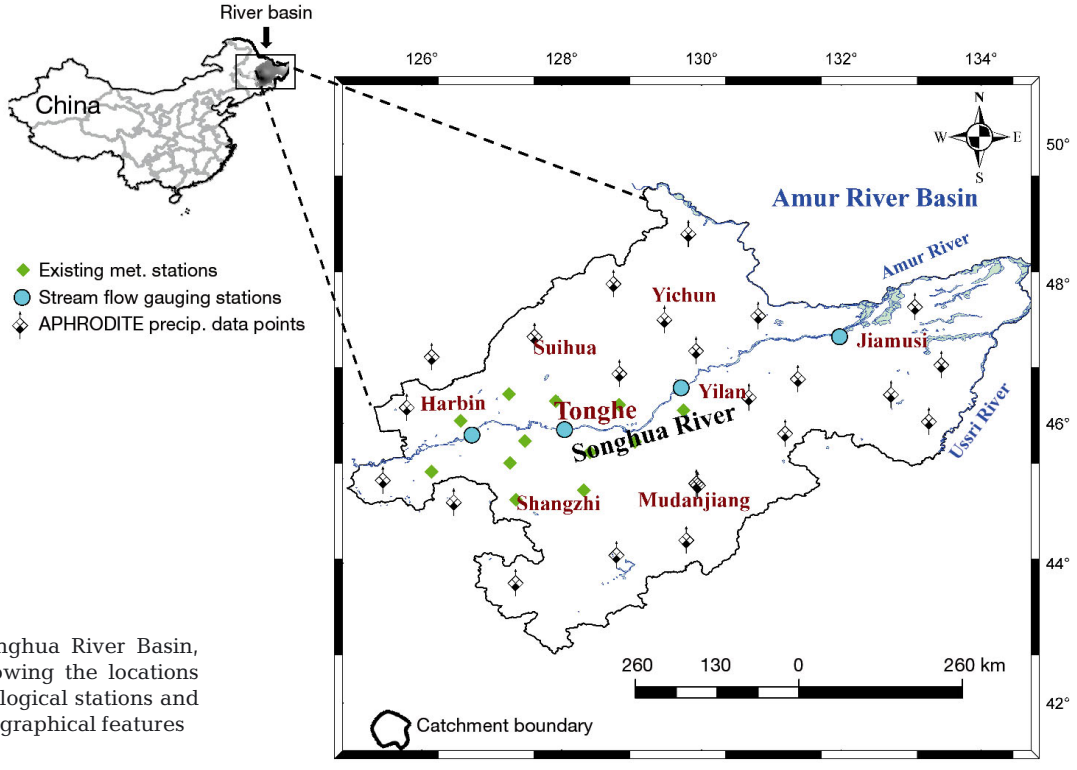

Fig. 1. Songhua River Basin, China, showing the locations of meteorological stations and some geographical features

Table 4. Details of meteorological stations and data (1961–2005) used in the analysis; NA: not applicable

Station no.	Station ID	Name	Latitude (°N)	Longitude (°E)
1	50953	Harbin	45.75	126.77
2	50963	Tonghe	45.95	128.03
3	50877	Yilan	45.38	126.3
4	50968	Shangzhi	45.97	128.73
5	NA	Mudanjiang[a]	44.53	129.60
6	NA	Yichun[a]	47.71	128.85
7	NA	Jiamusi[a]	46.78	130.33
8	NA	Suihua[a]	46.92	126.97

[a]Precipitation data not available (replaced by APHRODITE precipitation data product)

required to avoid negative effects of natural hazards, and to maintain agricultural production.

2.2. Data sets

Daily inputs of meteorological variables (minimum and maximum temperatures, precipitation, wind speed, relative humidity, sunshine hours, and pan evaporation) for 15 meteorological stations from 1961–2005 were provided by the Meteorological Administration of Heilongjiang Province, China. Data quality was previously assessed by the Meteorological Administration of Heilongjiang. Eight stations out of 15 that cover the whole period (1961–2005) were selected to study precipitation extremes and drought (Fig. 1, Table 4). APHRODITE gridded precipitation data, which have a resolution of 0.25° × 0.25°, from 25 different coordinates for the period, were also used, due to the limited availability of precipitation data. The gridded precipitation was defined by interpolating the station-based observations from regional hydrological and meteorological stations (Yatagai et al. 2009). APHRODITE precipitation data (APHRO_MA_V1101) have a coarse resolution; therefore, we assumed that precipitation is constant at any given elevation in the grid area.

A hierarchical cluster analysis was carried out for data from observations and the gridded precipitation product (APHRODITE precipitation) to validate the meteorological stations and selected coordinate points (Fig. 2). Clusters represent a perfect grouping of highly similar distribution patterns of the area, such as statistical (or stochastic), as well as physical and geographical features. After performing the clustering, the Kolmogorov-Smirnov test was also applied to assess the null hypothesis of a normal distribution. The test indicated that it was not possible to reject the null hypothesis of a normal distribution for the clustered stations. For observed and APHRODITE data, 3 and 4 clusters having similar statistical properties (coefficient of skewness and coefficient of kurtosis) were selected, respectively (Fig. 3). Six APHRODITE data points were removed due to large errors. Moreover, historical outputs for the period 1961–2005 for 11 GCMs released from different institutes were also downloaded from https://pcmdi.llnl.gov/mips/cmip5/, and these data were provided by the World Climate Research Program.

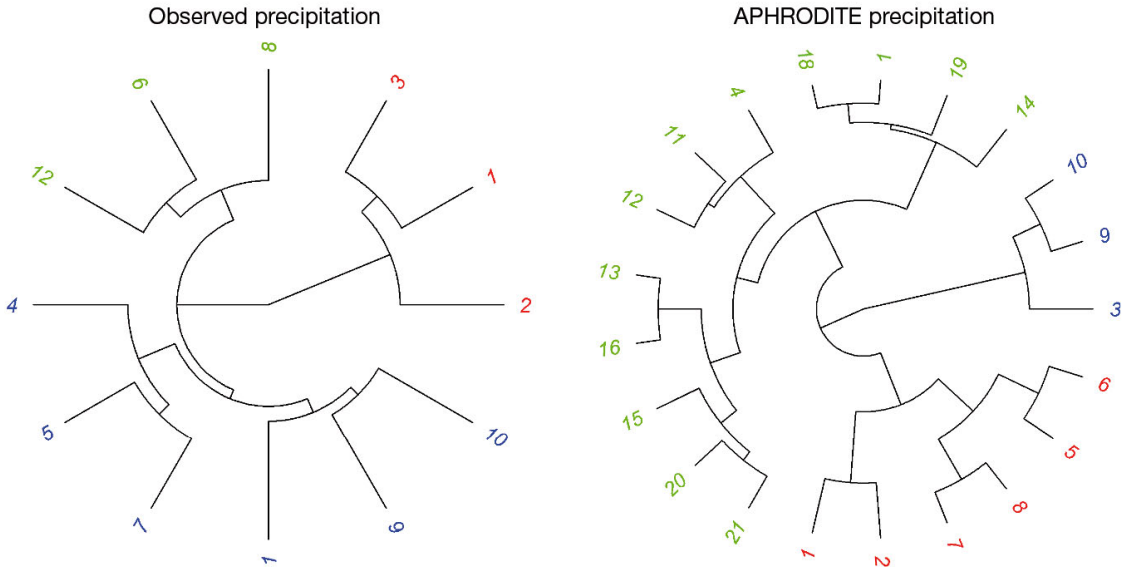

Fig. 2. Hierarchical cluster diagram for (a) observed precipitation and (b) spatial precipitation data. Different colors represent clusters

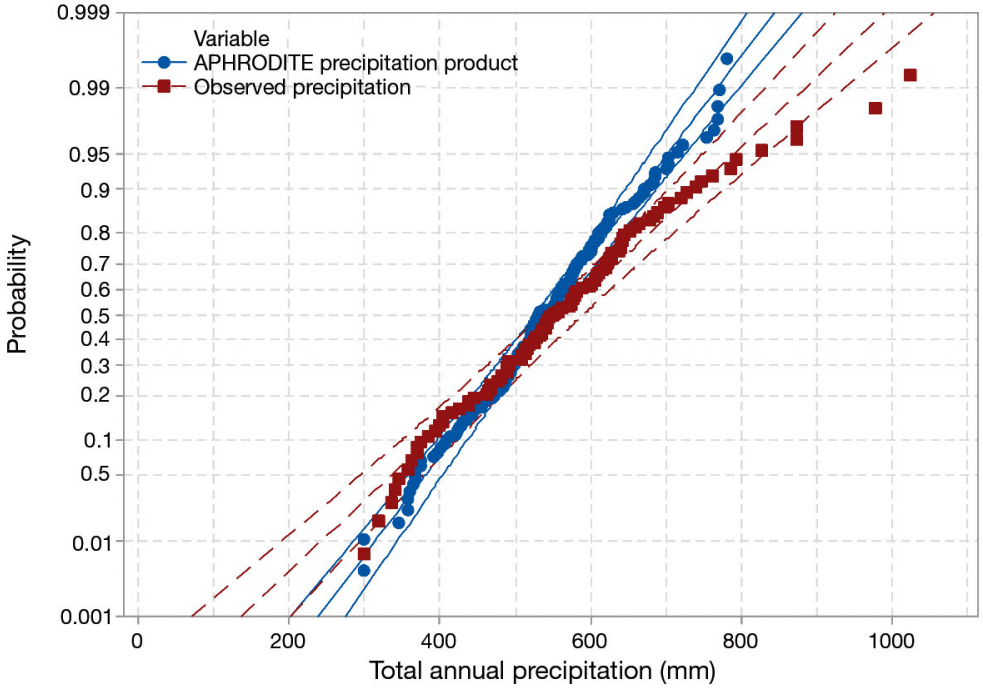

Fig. 3. Probability distribution plot for clustered precipitation data at 95% confidence intervals

3. METHODS

3.1. Selection of indices

3.1.1. Extreme precipitation indices

Seven extreme precipitation indices were selected from the primary list of indices recommended by the joint CCl/CLIVAR/JCOMM ETCCDI (http://etccdi.pacificclimate.org) for the present analysis. These indices were classified into 2 types. The first group includes precipitation indices (RX1day, PRCPTOT, R99, and SDII), whereas the second group assesses the number of rainy days (CDD, CWD, and R20mm). Details of these indices are provided in Table 2. These indices have been widely used to assess changes in extreme precipitation events because they have relatively low noise, weak extremes, and strong significance (Sillmann & Roeckner 2008, Li et al. 2013, Song et al. 2015).

3.1.2. Drought indices

Three drought indices (CI, RDI, and SPEI) were selected for drought monitoring. These indices can be used for regional and global-scale drought monitoring (Tsakiris & Vangelis 2005, Qian et al. 2007, Tsakiris et al. 2007, Vicente-Serrano et al. 2010, 2012a, Vangelis et al. 2013). Furthermore, these drought indices can provide comprehensible and transparent environmental information on drought for the general public (Monacelli et al. 2005). The CI is based on multiple scale standardized precipitation (SPI), precipitation amount, and relative soil moisture (M). In this study, CI is calculated by applying the method of Zou & Zhang (2008):

$$CI = a \times SPI_1 + b \times SPI_3 + c \times M \quad (1)$$

where a, b are normalized precipitation coefficients, and c is a relative humidity coefficient; values for these terms were set to be 0.4, 0.4, and 0.8, respectively, which were taken from Zou & Zhang (2008). These coefficients were obtained from the National Standard GB/T 20481-2006 of Meteorological Drought Grade (China). SPI_1 and SPI_3 were calculated from the recent 1 mo and recent 3 mo precipitation using SPI, following the methodology proposed by McKee et al. (1993). In Eq. (1), M is a relative soil moisture index, which is calculated as follows:

$$M = \frac{(P - ET_o)}{ET_o} \quad (2)$$

where P is precipitation and ET_o is reference evapotranspiration, which is calculated using the FAO-56 PM equation (Allen et al. 1998). For CI-Pan, ET_o is replaced by pan evaporation. For both standard CI and CI-Pan, values <–0.6 are considered to reflect a state of drought. The more severe the dry conditions, the smaller the value of the composite drought index

(Qian et al. 2011). Based on dry conditions, the normal drought condition is defined as CI > −0.6; light drought ranges between −1.2 and −0.6, and extreme drought is defined as CI ≤ −2.4, while moderate drought is indicated by CI values between −1.2 and −1.8, and extreme drought is indicated by CI values below −1.8, respectively.

The RDI is based on cumulative precipitation and potential evapotranspiration, and it can be calculated for any month k of the i^{th} year (Tsakiris et al. 2007):

$$a_k^i = \frac{\Sigma_{j=1}^{k} P_{ij}}{\Sigma_{j=1}^{k} \mathrm{PET}_{ij}} \quad (3)$$

where i = (1)1 and j = 1(1) k, a_k is the RDI value, P_{ij} is the cumulative precipitation that falls during the j^{th} month of the i^{th} year. PET_{ij} is the potential evapotranspiration that occurs during the j^{th} month of the i^{th} year, and it can be calculated by any of several methods, such the Hargreaves, Thornthwaite, and Blaney-Criddle formulas. For RDI-Pan, PET_{ij} is replaced by pan evaporation. Mathematically, RDI-Pan is similar to RDI, but RDI-Pan is based on pan evaporation and precipitation. Therefore, RDI-Pan employs the same standardized drought index categories as used by standard RDI. The standardized drought can be classified as mild (−0.5 to −1.0), moderate (−1.0 to −1.5), severe (−1.5 to −2.0), and extreme (<−0.2), respectively.

The complete theoretical background of SPEI is explained elsewhere (Vicente-Serrano et al. 2010, 2012a,b, Beguería et al. 2014). The SPEI combines monthly precipitation and evapotranspiration in a simple climatic water balance ($P - ET_o$). The 3-parameter log–logistic distribution is used to adjust this water balance. Negative (positive) values of SPEI represent dry (wet) conditions. In this study, the SPEI is also reformulated with reference evapotranspiration, and is adjusted with a 3 parameter log-logistic distribution.

The abovementioned indices (CI, RDI, and SPEI) were calculated using evapotranspiration estimated wind speed, minimum and maximum air temperature, net radiation, and relative humidity. However, FAO-56 PM needs additional inputs for CI, and this need for additional data complicates the use of CI in assessing drought events because of the non-availability of data. Moreover, the potential evapotranspiration used in RDI and SPEI is calculated using air temperature (Thornthwaite equation). This simplified method of calculating evapotranspiration for RDI and SPEI may produce biases due to global warming. These biases may cause overestimates of the drought episodes in the form of their durations, magnitude, intensity, and areal extent (Sheffield et al. 2012, B. Li et al. 2014). Therefore, in this article, the original indices are compared with the reformulated indices that use pan evaporation, reference evapotranspiration, and precipitation to identify possible drought episodes in the study area.

The indices CI and CI-Pan were calculated on a monthly scale (April–May–June) for the period 1961–2005, whereas RDI, RDI-Pan, RDI-PM, SPEI, and SPEI-PM were calculated on a 3 mo scale for the same time period using a basin-wide approach in the SRB. Theoretical distributions (normal and logistic) were used to assess the normal distribution patterns of drought episodes in the study area. The drought indices follow normal distributions in this region. Moreover, the Mann–Kendall trend test (Kendall 1975) was also applied to detect trends in the climate extremes.

3.2. Downscaling technique

The gridded GCM outputs were spatially downscaled to the scale of the study area by applying the generator for point climate change (Zhang 2005, Mullan et al. 2016). Due to its simplicity and ease of use, this method treats spatial and temporal variation separately. In addition, this method has an advantage over most statistical downscaling methods in that it can be used to downscale non-stationary climate (Zhang et al. 2012, Li et al. 2013). Moreover, the probability distributions of point data are used in this technique by exploiting the GCM outputs rather than the recognition of strong one-by-one correlations amid station values and GCM outputs.

In the first step, the daily GCM outputs were interpolated onto a common grid with a resolution of 0.5° × 0.5°. The bilinear interpolation method was applied using the Climate Data Operators command-line tools, which were downloaded from https://code.zmaw.de/projects/cdo. In the second step, the estimated linear and nonlinear transfer functions were applied to the gridded GCM data. The observations on the y-axis were plotted with the ranked GCMs (also called a qq-plot). Best-fit linear and nonlinear functions, called transfer functions, were obtained using LAB-fit software-Universidade Federal de Campina Grande, Brazil (Silva & Silva 2009). This curve-fitting software automatically generates 200 functions up to 4 fitting parameters and 1 independent variable, and makes a list of functions according to rank of the functions' residual errors. These functions were then applied to downscale the GCM out-

put to the scale of the study area to obtain means of downscaled values under different GCMs.

4. RESULTS

4.1. Performance of GCM-based indices and basin-wide trends in extreme precipitation indices on annual scales

The performance of the CMIP5 historical simulations using different GCMs is presented in Fig. 4. This comparison was made to evaluate the discrepancies between the downscaled simulations of the CMIP5 ensemble and observations. For this purpose, the Pearson correlation coefficient was calculated between the downscaled simulations of the CMIP5 ensemble and observations. The spatial correlation between the observations and the extreme indices from the downscaled model outputs (except R20mm) was never <0.80, which reflects a good performance of the downscaled simulations with respect to observations. In the case of R20mm, differences were found in the individual simulations, but the multi-model ensemble (MME) showed good agreement. The spatial correlation varied from 0.7 to 0.85. The above assessment indicates that the ensemble mean performs better than individual models. Based on the above scenario, the analysis below was performed using the CMIP5 ensemble mean.

Fig. 5 shows the basin-wide trend in annual extreme precipitation indices within the SRB for the period of 1961–2005. Most of the extreme precipitation indices showed negative and non-significant trends in the study area.

In the case of the *in situ* analyses, minimum values of PRCPTOT were found in the 1970s and 2000s. In the analysis of the inter-annual variability using PRCPTOT, a pattern of decline–increase–decline was observed. A peak value of 702 mm occurred in 1998 and a local minimum of 405 mm occurred in 2000, whereas a basin-wide increase of 1.9 mm yr^{-1} was found for the entire area. The MME indicated a lower peak value of 598 mm in 1998 and a regionally averaged value of 1.23 mm yr^{-1} compared to the *in situ* measurements. However, the trend was not significant at the 0.05 level. In both cases (*in situ* and MME) during the whole period (1961–2005), a non-significant decreasing trend at the 0.05 level was found in SDII, which had a slope of 0.033 mm yr^{-1}. During the annual analysis, it was also observed that from 1961–2000, RX1day and R99 showed variations that were similar to those of PRCPTOT. In the case of *in situ* RX1day and R99, no obvious trend was noted in the study area. However, the MME showed negative and non-significant trends at the 0.05 level with slopes of 0.29 and 0.002 mm yr^{-1} for R99 and RX1day, respectively.

4.2. Station-by-station trends in extreme precipitation indices on annual scales

Station-based analysis was also carried for the period 1961–2005 to determine the magnitude of extreme precipitation at every station in the river basin (Fig. 6). The results indicated that most of the *in situ* and MME-based PRCPTOT records showed significant increases in the region, whereas only 1 station (Shangzhi) experienced a non-significant decreasing trend. For R99, during the same time period, a positive non-significant trend at the 0.05 level was observed. For SDII and RX1day, 4 out of 7 stations experienced a downward trend, while the remaining 3 stations exhibited a non-significant positive trend at the 0.05 level. During the same time period, 3 of 7 stations recorded negative trends in R20mm and CWD, whereas the remaining stations showed non-significant increasing trends in the basin. For CDD, all stations exhibited positive upward trends over the entire study area. Song et al. (2015) also confirmed that 79–82% of the stations exhibited positive trends in PRCPTOT and R99, whereas 49% of the stations reflected negative trends in SDII during the period 1960–2013 in the SRB. Overall, the trend magnitude of PCRPTOT was larger than that of other extreme precipitation indices. In the case of MME, the station-based results were comparable with those of *in situ* extreme precipitation indices, and very small differences were found during the whole analysis (Fig. 6). In this analysis, R20mm showed high variability compared to the other indices with different magnitudes. In the 1970s and the 1990s, 7 and 6 very heavy rainfall days occurred in the basin, respectively. In 1998, an extreme precipitation event (flood) occurred in the basin. CWD showed a decreasing trend compared to CDD. The *in situ* stations showed no trend, whereas the MME captured a negative non-significant trend at the 0.05 level with a slope of 0.003 d yr^{-1}. In the case of CDD, the *in situ* stations and MME both accurately showed the number of dry days that occurred during the time period 1961–2005 with the slope of 0.33 d yr^{-1} at the 0.05 level (Fig. 7). The above analysis showed that all of the SRB experienced a drier situation during the whole time period (1961–2005).

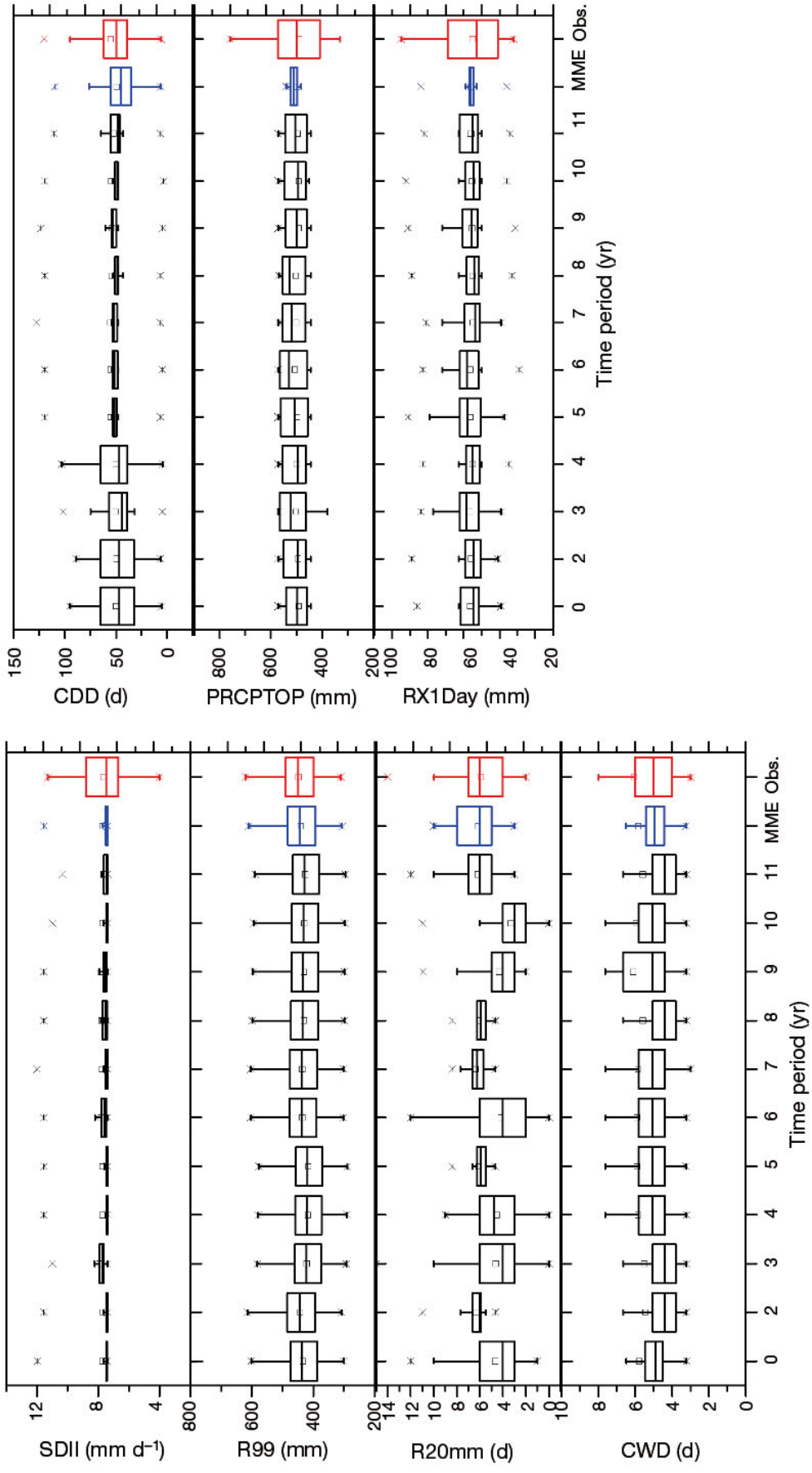

Fig. 4. Comparisons of model simulations and observations of climate extremes for the period 1961–2005. Indices are defined as in Table 2. MME: multi-model ensemble, Obs.: observation. Box plots—small box: mean; horizontal line: median; whiskers: interquartile range; asterisks: minimum and maximum values

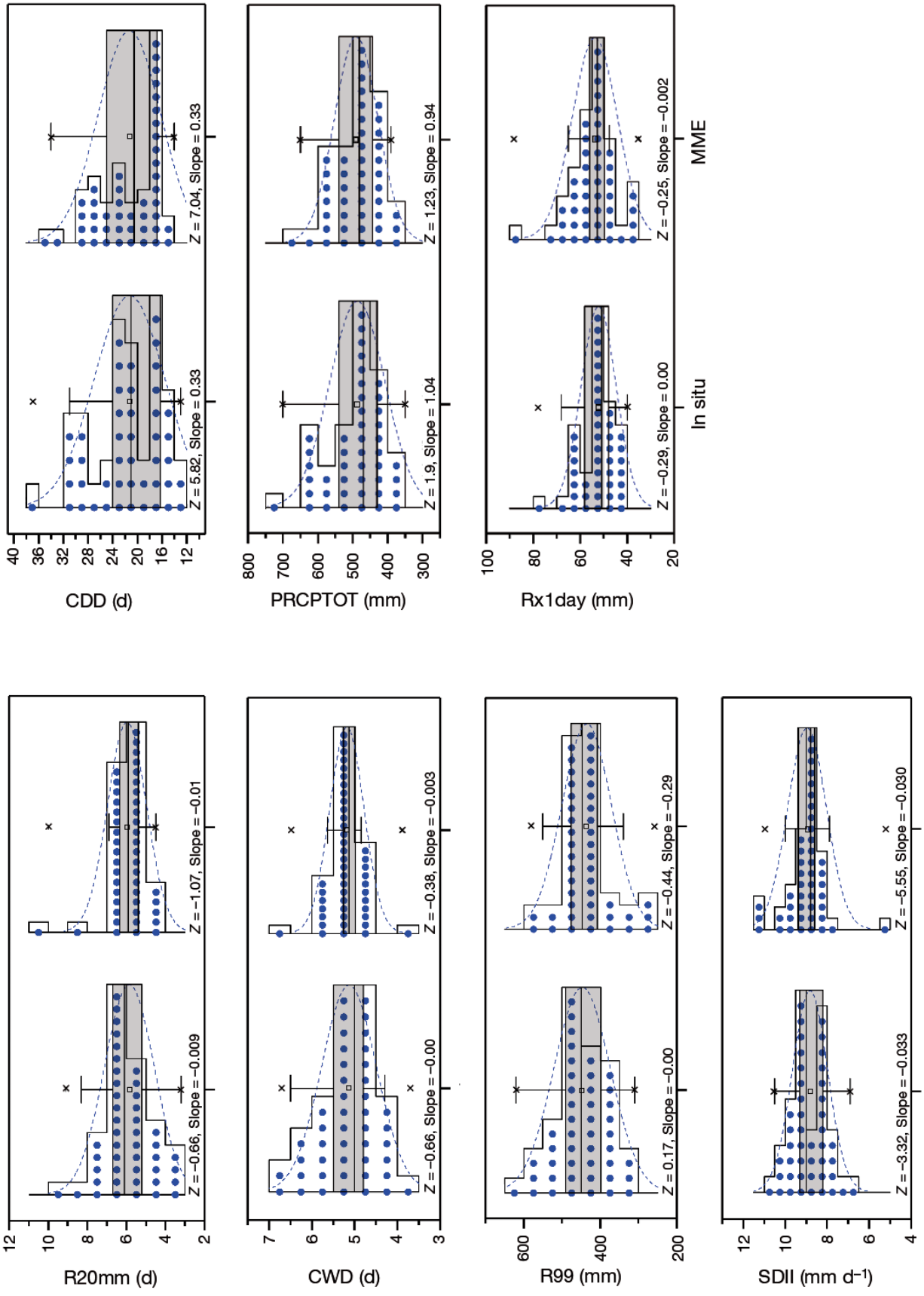

Fig. 5. Trends of extreme precipitation in the Songhua River Basin for the period 1961–2005, as measured at *in situ* stations and from multi-model ensemble (MME) means. Bars and blue curve: normal distribution of extreme indices in the basin. Box plots (shaded grey) — left: annual linear trends in extreme precipitation at *in situ* stations; right: as with left plots, but obtained from the general circulation models using the MME. Small box: mean; horizontal line: median; whiskers: interquartile range; ×: minimum and maximum values; blue dots: data points. Indices are defined as in Table 2

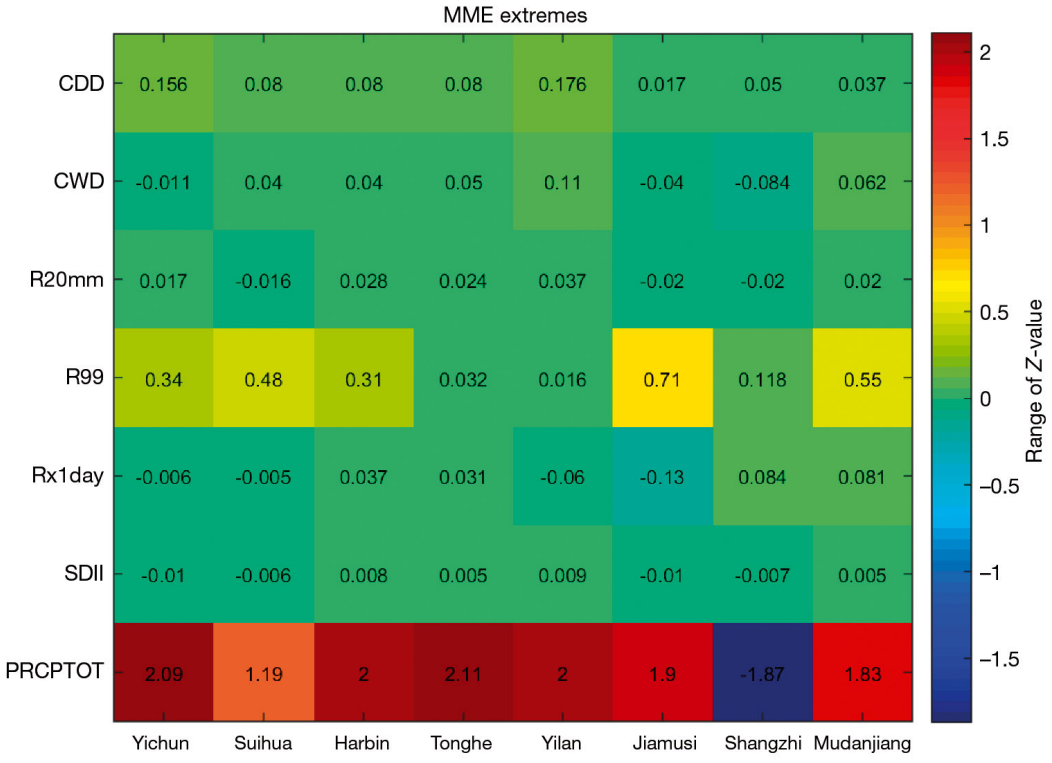

Fig. 6. Station-wise *Z*-values and trends of extreme precipitation indices using CMIP5 ensemble mean data from 1961–2005

4.3. Comparison of drought indices

The drought indices (CI, RDI, SPEI, CI-Pan, RDI-Pan, SPEI, SPEI-PM, and RDI-PM) were applied to the period 1961–2005 to characterize drought and perform a comparison of the drought indices in the SRB. Three stations, Harbin, Yilan, and Jiamusi, which lie along the upper, middle, and lower reaches of the main stream of the Songhua River, respectively, were selected to assess the impact of historical

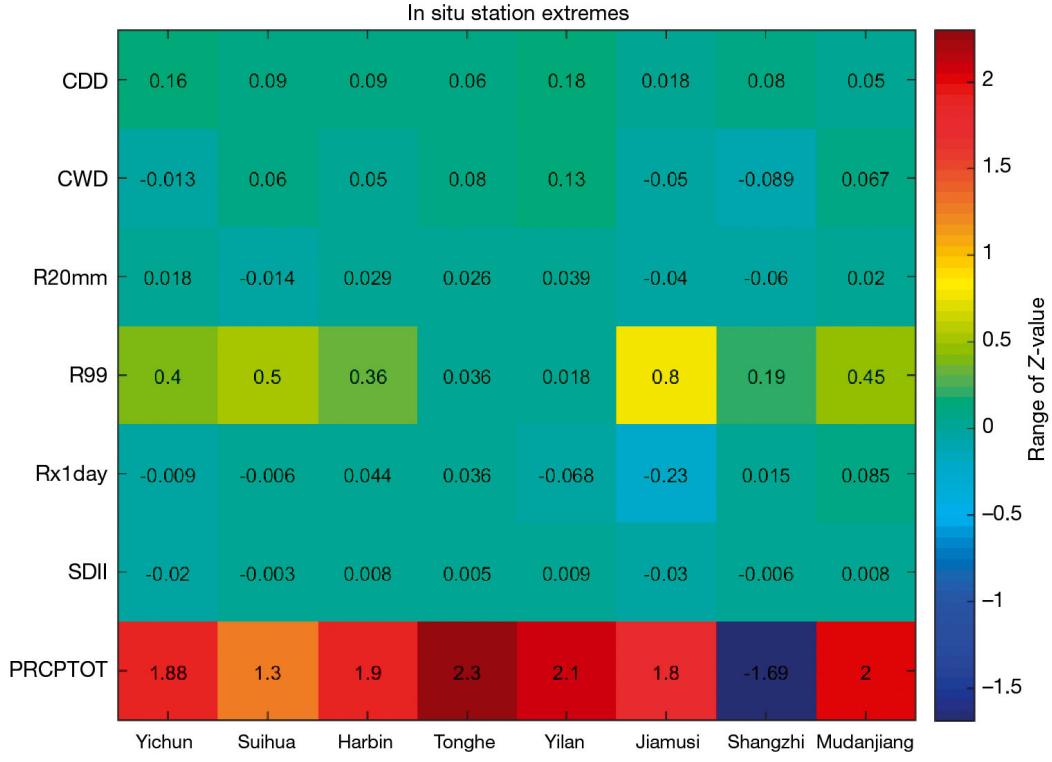

Fig. 7. Station-wise *Z*-values and trends of extreme precipitation indices using observed data from 1961–2005

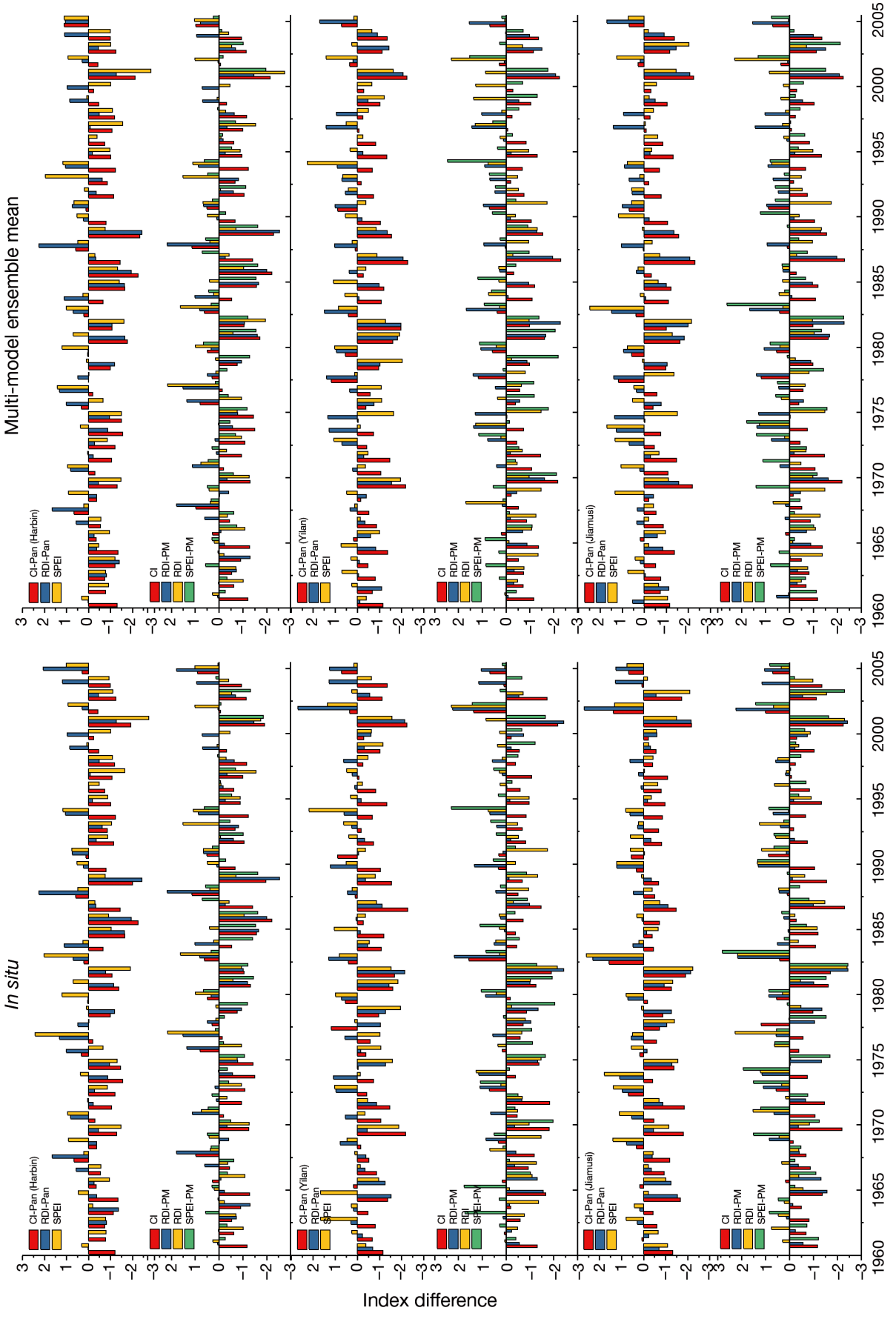

Fig. 8. Comparison of drought indices at Harbin, Yilan, and Jiamusi stations. Indices are defined as in Table 2. Left column: *in situ* stations, right column: multi-model ensemble mean

drought events (Fig. 1). The comparison of the drought indices for the abovementioned stations is presented in Fig. 8. For the 1970s, all indices reflected mild to moderate drought at Harbin station. In the 1980s, CI, RDI-PM, and SPEI-PM showed severe drought years (1985, 1986, and 1989), whereas RDI and SPEI showed mild to moderate drought during the same time period. In the 1990s, mild to moderate drought occurred over the whole time period at Harbin station. By replacing reference evapotranspiration with pan evaporation, CI and CI-Pan showed the same results and yielded different drought magnitudes, but RDI-Pan, RDI-PM, and SPEI-PM indicated an extreme drought year in 1991. The trend of precipitation extremes also indicated that during the time period 1961–2005, more dry days were recorded than wet days. The RX1day and R99 also showed non-significant trends in the basin. This scenario indicates that during the whole time period, the occurrence of light precipitation was larger compared to heavy precipitation in the study area. During the rainy season, less intense precipitation needs more time to penetrate the soil, which results in low runoff. Consequently, less intense precipitation results in fewer wet days. Moreover, F. Li et al. (2014) found a significant increase in mean annual temperature during 1960–1990 and an abrupt rise after the 1990s compared to previous time periods. The increased temperature enhanced the evaporation demand, leading to a reduction of soil moisture and consequently, intense drought (Douville et al. 2002). It may also be concluded that although extreme precipitation events such as the 1998 flood occurred in the region, overall precipitation was reduced in the SRB. Based on previous publications and recommendations from the FAO, the FAO-PM equation is the standard method and the most accurate estimation of evapotranspiration despite the availability of data.

In the case of standard RDI and SPEI, evapotranspiration was measured using air temperature (Thornthwaite method), so the standard RDI exhibited different results compared to the SPEI-PM. The upper and middle stations along the Songhua River showed that the standard CI, CI-Pan, RDI-Pan, RDI-PM, SPEI, and SPEI-PM well captured severe drought years. CI, CI-Pan, RDI-Pan, and RDI-PM indicated severe drought in 1981, 1982, 1987, and 2001, whereas the standard RDI and SPEI captured 2 extreme and 1 severe drought during that time period. For the MME, the drought indices showed comparable results with those from the *in situ* stations. During the analysis, a small discrepancy in the results from the MME was found. For example, SPEI-PM captured more severe drought years at Yilan station compared to other indices. The differences between the indices based on evapotranspiration and those based on evaporation are presented in Fig. 9. The results indicate that the performance of all indices is better than that of the standard RDI. The difference in the ability of CI and SPEI to capture drought is large compared to RDI. The composite index and SPEI indicates severe drought, while RDI indicates moderate drought. The performance of the drought indices was assessed comparing the time-series of SPEI, RDI, and CI with relative soil moisture with 2 layers, i.e. 18 and 28 cm, for 2 locations in the SRB. Relative soil moisture data were downloaded from http://climate.envsci.rutgers.edu/soil_moisture/19yrchina.htm for the years 1981–1999 and from the China Meteorological Administration for the years 2000–2005.

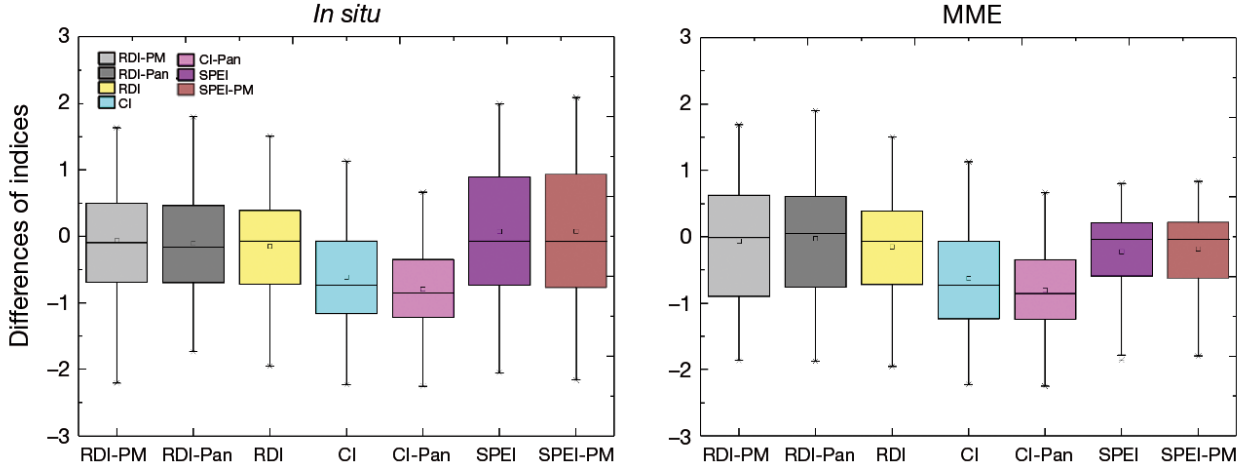

Fig. 9. Distribution differences between drought indices. Indices are defined as in Table 2. Left: *in situ* stations, right: multimodel ensemble mean. Box plots — small box: mean; horizontal line: median; whiskers: interquartile range; asterisks: minimum and maximum values

Table 5. Correlation between relative soil moisture in 2 layers and the drought indices (1981–2005). CI: composite index; RDI: reconnaissance drought index, SPEI: standardized precipitation evapotranspiration index; suffixes '-Pan' and 'PM' indicate indices reformulated using pan evaporation and Penman–Monteith equations, respectively

Station	Soil layer (cm)	CI	CI-Pan	RDI-Pan	RDI	RDI-PM	SPEI	SPEI-PM
Harbin	18	0.23	0.19	0.22	0.16	0.24	0.01	0.005
	28	0.32	0.30	0.29	0.30	0.32	0.30	0.36
Jiamusi	18	0.24	0.25	0.20	0.08	0.25	0.02	0.12
	28	0.02	0.16	0.002	0.15	0.05	0.000	0.004

A correlation analysis (Kendall 1975) was performed between the drought indices and the relative soil moisture in 2 layers (18 and 28 cm) at Harbin and Jiamusi stations (Table 5). The results show that the indices using the PM equation for calculating potential evapotranspiration are more significant than the evapotranspiration estimates made using the Thornthwaite equation. The RDI and SPEI showed lower correlation compared to composite indices, RDI-PM and SPEI-PM. During analysis, it was noted that the RDI and SPEI computed with PM-ET_o better correlated with soil moisture, and Thornthwaite was the least suitable method to depict soil moisture. However, the PM-ET_o provided small correlation with observed soil moisture, which is always better than correlations between the soil moisture data and the drought indices computed with Pan. This lower correlation also indicates that potential evapotranspiration estimates made using air temperature may contain biases, due to global warming. From 1965–2013, a rise in temperature (1.2 to 2.2°C) in the Sangjiang Plain (a subcatchment of the SRB) was confirmed by Yan et al. (2003). Wang & Zhang (2011) also documented that the 1990s was the warmest period that has occurred in China. Warming may create the possibility that RDI will capture fewer drought events, and the correlation among the indices will be reduced.

A regional average drought analysis was also carried out on a monthly basis to compare with extreme precipitation. The maximum 1 d precipitation and reformulated indices with pan evaporation were selected for this comparison because RX1day displays the same variation compared to the other extreme precipitation indices, such as R99 and PRCPTOT. During this analysis, it was observed that peak precipitation days occur in July and August, while April and September are associated with drought conditions during 1961–2005 (Fig. 10). The results indicate that most of the drought events occur in spring (April and May) and fall (September and October) in the SRB.

4.4. Station-by-station evaluation of drought indices

Station-by-station evaluation of drought indices was also carried out to identify the drought events in the SRB. Standard CI and CI-Pan captured 2 extreme

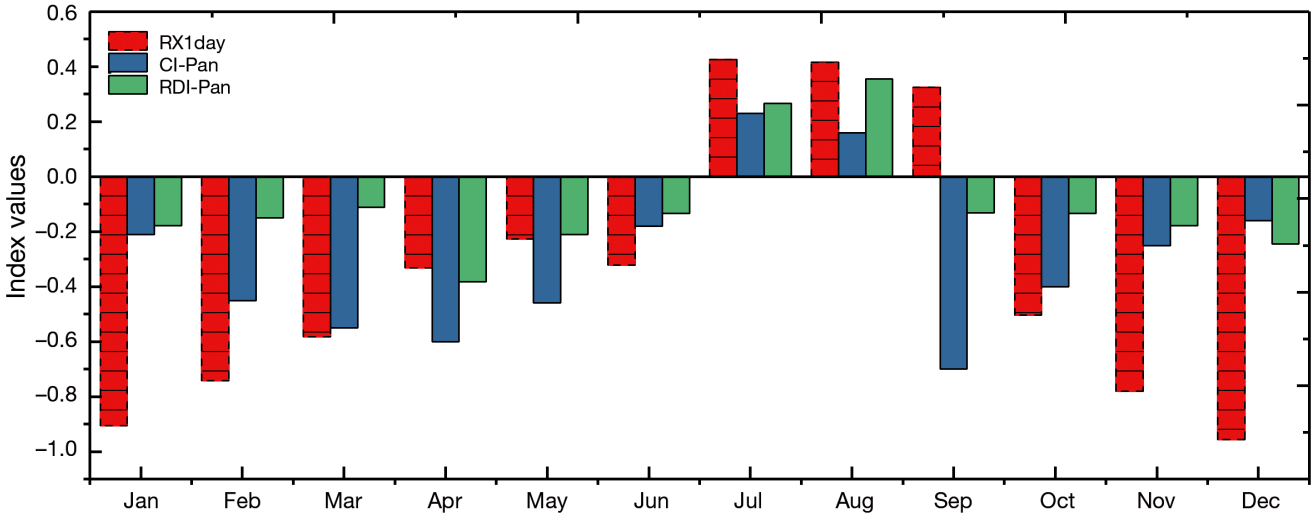

Fig. 10. RX1day, the composite index with reformulation of the pan evaporation equation (CI-Pan), and the reconnaissance drought index with reformulation of the pan evaporation equation (RDI-Pan) on a monthly scale from 1961–2005

and 6 severe drought events at Mudanjiang and 4 severe events at Shangzhi, respectively, whereas the standard RDI and RDI-Pan captured only 2 extreme drought events with magnitudes of <–2.0 during the whole time period at Mudajiang and Shangzhi stations. On the other hand, SPEI captured 2 severe droughts at Mudanjiang and 2 extreme and 2 severe drought events at Shangzhi station, respectively. During analysis, it was also observed that using the PM equation, the RDI-PM exhibited different results as compared to standard and reformulated indices. The RDI-PM captured 2 extreme and 4 severe drought events while SPEI-PM captured 7 severe drought events at Mudanjiang station. For Suihua and Tonghe stations, CI and CI-Pan captured 3 extreme drought events with a magnitude <–2.1, whereas the standard RDI, RDI-Pan, and RDI-PM also captured 3 drought events with a magnitude <–2.2 during the 45 yr time period (Fig. 11). The reformulated SPEI captured different drought events during the same time period. For example, SPEI captured 2 severe drought events, while SPEI-PM captured 3 severe events at Suihua station. For Tonghe station, SPEI and SPEI-PM captured the same drought events but with different magnitude. During 1982, RDI and RDI-Pan showed extreme drought, but other indices indicated a severe drought at Suihua station. RDI-PM and SPEI-PM showed good agreement compared to the standard RDI for all stations. These differences may be due to the simple method (i.e. temperature based) of estimation of potential evapotranspiration by RDI.

5. DISCUSSION

Recent studies have shown that, in most parts of the world, the intensity and frequency of precipitation events are increasing (Derbyshire 2001, Sen Roy & Balling 2004, Modarres & Sarhadi 2009, Fu et al. 2013). The current analysis has shown that SRB also exhibits an upward trend with a small magnitude in terms of extreme precipitation. These results are comparable with worldwide research and literature (Frich et al. 2002, Klein Tank & Können 2003, Goswami et al. 2006, Fu et al. 2010). Furthermore, the GCM-based calculated indices showed the same results as the *in situ* stations. In addition, northeastern China experienced extreme precipitation events during the flood period (July) (Yang et al. 2008). In our case, the SRB also experienced an increase in the frequency of R99 during the period 1961–1990. The results indicate that precipitation displayed a negative–positive trend. For example, from 1961–1980, a negative trend was identified in the SRB, and a positive trend was identified after 1980. Moreover, the extreme precipitation indices also showed the same results, except for PRCPTOT. The results are comparable with a previous study that reported positive–negative trends in mean annual precipitation in northeastern China (Sun et al. 2000). The SDII showed upward–downward variations that are comparable with those reported by regional studies, such as on the Loess Plateau and in Shaanxi Province (Li et al. 2010, Liu et al. 2013).

The current analysis also indicates that CDDs have increased over the study area, which may cause severe droughts. Liu et al. (2009) and Zhang et al. (2011) also reported droughts during the plant growth period in the Songnen Plains and Northeast China. Lack of precipitation causes discontinuity of the Taoer River, which is a tributary of the Songhua River (Liang et al. 2008).

The above discussion indicates that observations and GCM output display small variations in the results, which may be due to downscaling or the coarse resolution of the GCMs. Moreover, pan evaporation-based drought indices identify drought events with better agreement compared to standard drought indices, but future studies are still required for improvement of this method using other climatic variables.

6. CONCLUSIONS

The current analysis was carried out to examine trends in extreme precipitation and drought events using standard and reformulated drought indices based on pan evaporation for the period 1961–2005. Historical outputs from CMIP5 simulations were also used to identify the discrepancies between the GCMs. The results showed that, in the past 45 yr, PRCPTOT increased over the entire study area, whereas SDII showed an upward, followed by a downward trend. The RX1day, R20mm, and CWD indices did not show any trends. For CDD, the entire study area exhibited an upward trend. During the analysis, very small differences were found between the extreme precipitation indices calculated for the MME and the *in situ* stations.

The reformulated drought indices enhanced the performance of drought indices in monitoring drought events in the study area. CI and CI-Pan indicated that the spring and fall seasons are associated with drought during the whole study period. A compari-

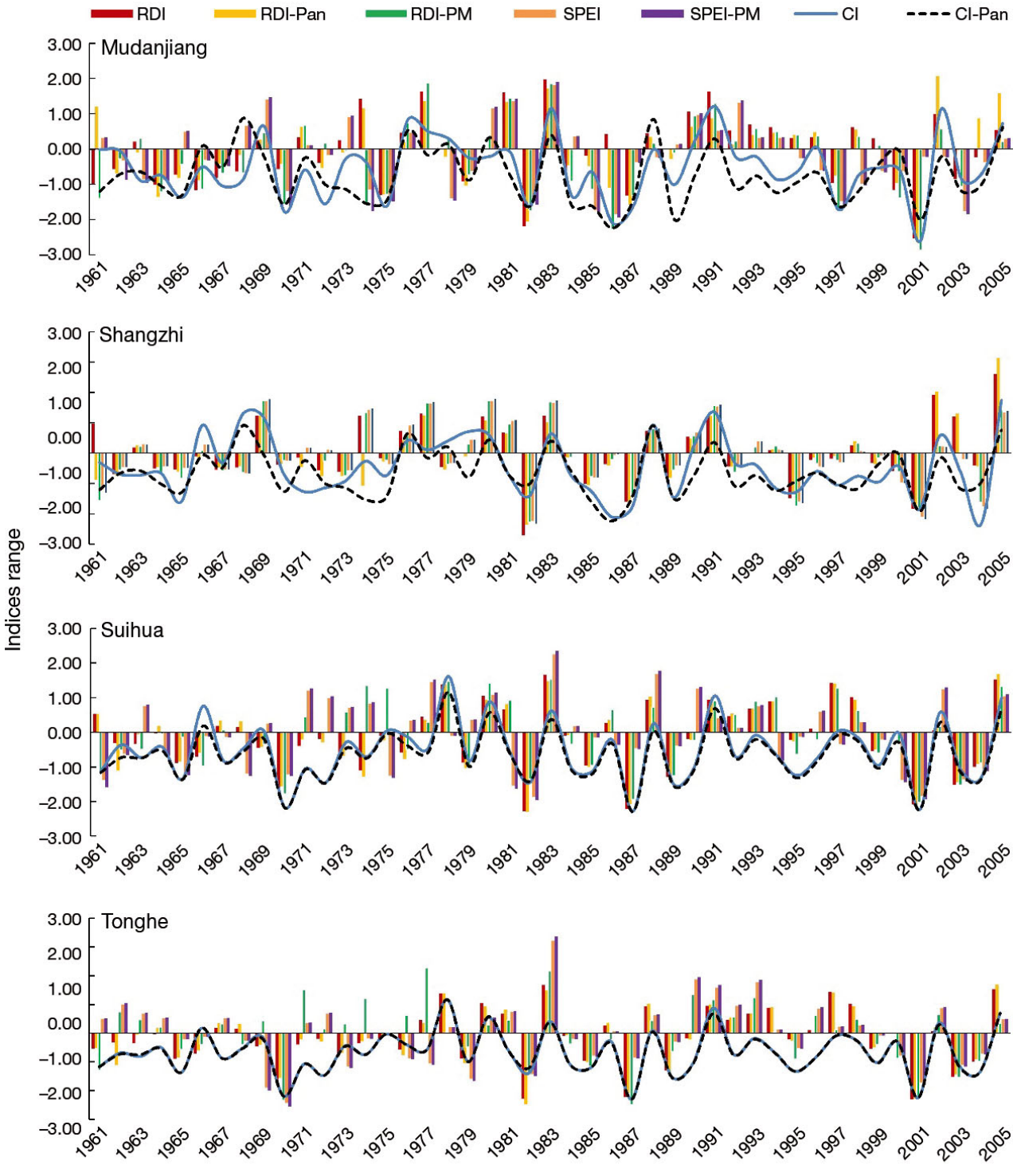

Fig. 11. Station-wise performance of drought indices in the Songhua River Basin

son of the indices showed that the performance of CI, CI-Pan, RDI-PM, and SPEI-PM is better than that of standard RDI and SPEI for every station. Overall, the entire study area experienced severe drought during the years 1970, 1987, and 2001. The correlation analysis between drought indices and observed soil moisture indicated that the RDI and SPEI computed with PM-ET_o better correlates with soil moisture than when computed with the Thornthwaite method. The results also suggest that the selection of the evapo-

transpiration estimation method is more important to accurately explain soil moisture than the drought index used in the study area.

The above analysis is based on a simple modification to the drought indices. The results are comparable with those of other studies. However, additional work is required to identify the influence of climate variables on evaporation when combined with the drought indices.

Acknowledgements. This study was supported by the National Natural Science Foundation of China (nos. 51579044, 41071053, and 51479032), National Key R&D Program of China (no. 2017YFC0406002), Natural Science Foundation of Heilongjiang Province (no. E2017007), and the Science and Technology Program of Water Conservancy of Heilongjiang Province (nos. 201319, 201501, 201503).

LITERATURE CITED

Allen RG, Jensen ME, Wright JL, Burman RD (1989) Operational estimates of reference evapotranspiration. Agron J 81:650–662

Alexander LV, Zhang X, Peterson TC, Caesar J and others (2006) Global observed changes in daily climate extremes of temperature and precipitation. J Geophys Res Atmos 111:D05109

Banimahd SA, Khalili D (2013) Factors influencing Markov chains predictability characteristics, utilizing SPI, RDI, EDI and SPEI drought indices in different climatic zones. Water Resour Manag 27:3911–3928

Beguería S, Vicente-Serrano SM, Reig F, Latorre B (2014) Standardized precipitation evapotranspiration index (SPEI) revisited: parameter fitting, evapotranspiration models, tools, datasets and drought monitoring. Int J Climatol 34:3001–3023

Beniston M, Stephenson DB, Christensen OB, Ferro CAT and others (2007) Future extreme events in European climate: an exploration of regional climate model projections. Clim Change 81:71–95

Boccolari M, Malmusi S (2013) Changes in temperature and precipitation extremes observed in Modena, Italy. Atmos Res 122:16–31

Bochetti MJ, Muñoz E, Tume P, Bech J (2016) Analysis of three indirect methods for estimating the evapotranspiration in the agricultural zone of Chillán, Chile. Obras Proy 19:74–81

Bouchet RJ (1963) Evapotranspiration réelle et potentielle, signification climatique. IAHS Publ 62:134–142

Brutsaert W, Parlange MB (1998) Hydrologic cycle explains the evaporation paradox. Nature 396:30

Chattopadhyay N, Hulme M (1997) Evaporation and potential evapotranspiration in India under conditions of recent and future climate change. Agric For Meteorol 87: 55–73

Christiansen JE (1968) Pan evaporation and evapotranspiration from climatic data. J Irrig Drain Div 94:243–266

Cohen S, Ianetz A, Stanhill G (2002) Evaporative climate changes at Bet Dagan, Israel, 1964-1998. Agric Meteorol 111:83–91

Cohen J, Screen JA, Furtado JC, Barlow M and others (2014) Recent Arctic amplification and extreme mid-latitude weather. Nat Geosci 7:627–637

Cong ZT, Yang DW, Ni GH (2009) Does evaporation paradox exist in China? Hydrol Earth Syst Sci Discuss 13:357–366

Derbyshire E (2001) Geological hazards in loess terrain, with particular reference to the loess regions of China. Earth Sci Rev 54:231–260

Douville H, Chauvin F, Planton S, Royer JF, Salas-Mélia D, Tyteca S (2002) Sensitivity of the hydrological cycle to increasing amounts of greenhouse gases and aerosols. Clim Dyn 20:45–68

Faiz MA, Liu D, Fu Q, Uzair M and others (2017) Stream flow variability and drought severity in the Songhua River Basin, Northeast China. Stoch Environ Res Risk Assess, doi:10.1007/s00477-017-1463-3

Frich P, Alexander LV, Della-Marta P, Gleason B, Haylock M, Klein Tank AMG, Peterson T (2002) Observed coherent changes in climatic extremes during the second half of the twentieth century. Clim Res 19:193–212

Fu G, Viney NR, Charles SP, Liu J (2010) Long-term temporal variation of extreme rainfall events in Australia: 1910–2006. J Hydrometeorol 11:950–965

Fu G, Yu J, Yu X, Ouyang R and others (2013) Temporal variation of extreme rainfall events in China, 1961–2009. J Hydrol (Amst) 487:48–59

Goswami BN, Venugopal V, Sengupta D, Madhusoodanan MS, Xavier PK (2006) Increasing trend of extreme rain events over India in a warming environment. Science 314:1442–1445

Guo J, Guo S, Li Y, Chen H, Li T (2013) Spatial and temporal variation of extreme precipitation indices in the Yangtze River basin, China. Stochastic Environ Res Risk Assess 27:459–475

Hao Z, AghaKouchak A (2013) Multivariate Standardized Drought Index: a parametric multi-index model. Adv Water Resour 57:12–18

Hargreaves GH, Samani ZA (1985) Reference crop evapotranspiration from temperature. Appl Eng Agric 1:96–99

IPCC (2013) Climate change 2013: the physical science basis. Contribution of Working Group I to the Fifth Assessment Report of the Intergovernmental Panel on Climate Change. Cambridge University Press, Cambridge

Kendall M (1975) Multivariate analysis. Charles Griffin, High Wycombe

Khan MI, Liu D, Fu Q, Dong S and others (2016) Recent climate trends and drought behavioral assessment based on precipitation and temperature data series in the Songhua River basin of China. Water Resour Manag 30: 4839–4859

Klein Tank AMG, Können GP (2003) Trends in indices of daily temperature and precipitation extremes in Europe, 1946–99. J Clim 16:3665–3680

Li B, Liang Z, Yu Z, Acharya K (2014) Evaluation of drought and wetness episodes in a cold region (Northeast China) since 1898 with different drought indices. Nat Hazards 71:2063–2085

Li F, Zhang G, Xu YJ (2014) Spatiotemporal variability of climate and streamflow in the Songhua River Basin, northeast China. J Hydrol (Amst) 514:53–64

Li J, Zhang Q, Chen YD, Singh VP (2013) GCMs-based spatiotemporal evolution of climate extremes during the 21st century in China. J Geophys Res Atmos 118:11017–11035

Li Z, Zheng F, Liu W, Flanagan DC (2010) Spatial distribution and temporal trends of extreme temperature and

precipitation events on the Loess Plateau of China during 1961–2007. Quat Int 226:92–100
Liang L, Li L, Zhang L, Li J, Li B (2008) Sensitivity of Penman-Monteith reference crop evapotranspiration in Tao'er River Basin of northeastern China. Chin Geogr Sci 18:340–347
Liang L, Li L, Liu Q (2011) Precipitation variability in Northeast China from 1961 to 2008. J Hydrol 404:67–76
Liu B, Xu M, Henderson M, Gong W (2004) A spatial analysis of pan evaporation trends in China, 1955–2000. J Geophys Res Atmos 109:D15102
Liu D, Luo M, Fu Q, Zhang Y and others (2016) Precipitation complexity measurement using multifractal spectra empirical mode decomposition detrended fluctuation analysis. Water Resour Manag 30:505–522
Liu W, Zhang M, Wang S, Wang B, Li F, Che Y (2013) Changes in precipitation extremes over Shaanxi Province, northwestern China, during 1960-2011. Quat Int 313–314:118–129
Liu XM, Li J, Lu ZH, Liu M, Xing WR (2009) Dynamic changes of composite drought index in Liaoning Province in recent 50 years. Shengtaixue Zazhi 28:938–942
Marengo JA, Jones R, Alves LM, Valverde MC (2009) Future change of temperature and precipitation extremes in South America as derived from the PRECIS regional climate modeling system. Int J Climatol 29:2241–2255
Martinez CJ, Thepadia M (2010) Estimating reference evapotranspiration with minimum data in Florida. J Irrig Drain Eng 136:494–501
May W (2008) Potential future changes in the characteristics of daily precipitation in Europe simulated by the HIRHAM regional climate model. Clim Dyn 30:581–603
McKee TB, Doesken NJ, Kleist J (1993) The relationship of drought frequency and duration to time scales. In: Proc 8th Conf on Applied Climatology. American Meteorological Society, Boston, MA, p 179–183
Mehran A, Aghakouchak A, Phillips TJ (2014) Evaluation of CMIP5 continental precipitation simulations relative to satellite-based gauge-adjusted observations. J Geophys Res 119:1695–1707
Modarres R, Sarhadi A (2009) Rainfall trends analysis of Iran in the last half of the twentieth century. J Geophys Res Atmos 114:D03101
Monacelli G, Galluccio MC, Abbafati M (2005) Drought assessment and forecasting. Drought within the context of region VI. Working group on hydrology, WMO, Průhonice
Mullan D, Chen J, Zhang XJ (2016) Validation of non-stationary precipitation series for site-specific impact assessment: comparison of two statistical downscaling techniques. Clim Dyn 46:967–986
Palmer WC (1965) Meteorological droughts. Res Pap 45. US Department of Commerce Weather Bureau, Washington, DC
Peterson TC, Golubev VS, Groisman PY (1995) Evaporation losing its strength. Nature 377:687
Qian W, Lin X (2005) Regional trends in recent precipitation indices in China. Meteorol Atmos Phys 90:193–207
Qian W, Fu J, Yan Z (2007) Decrease of light rain events in summer associated with a warming environment in China during 1961–2005. Geophys Res Lett 34:L11705
Qian W, Shan X, Zhu Y (2011) Ranking regional drought events in China for 1960–2009. Adv Atmos Sci 28: 310–321
Ratan R, Venugopal V (2013) Wet and dry spell characteristics of global tropical rainfall. Water Resour Res 49: 3830–3841
Ravazzani G, Corbari C, Morella S, Gianoli P, Mancini M (2012) Modified Hargreaves-Samani equation for the assessment of reference evapotranspiration in Alpine river basins. J Irrig Drain Eng 138:592–599
Ren GY, Guo J (2006) Change in pan evaporation and the influential factors over China: 1956–2000. Ziran Ziyuan Xuebao 21:31–44
Ren X, Martins DS, Qu Z, Paredes P, Pereira LS (2016) Daily reference evapotranspiration for hyper-arid to moist subhumid climates in Inner Mongolia, China. II. Trends of ETo and weather variables and related spatial patterns. Water Resour Manag 30:3793–3814
Roderick ML, Farquhar GD (2002) The cause of decreased pan evaporation over the past 50 years. Science 298: 1410–1411
Sen Roy S, Balling RC (2004) Trends in extreme daily precipitation indices in India. Int J Climatol 24:457–466
Sheffield J, Wood EF, Roderick ML (2012) Little change in global drought over the past 60 years. Nature 491:435–438
Shen SM, Qiao Q, Zeng ZS (1980) Moisture regime in black soils in northern part of north-east China. 3. Reliability of water supply for crop growth and the forecast of spring drought in the region of black soils. Turang Xuebao 17: 203–216
Sillmann J, Roeckner E (2008) Indices for extreme events in projections of anthropogenic climate change. Clim Change 86:83–104
Silva WP, Silva C (2009) LAB Fit curve fitting software: nonlinear regression and treatment of data program v. 7.2. 42. http://zeus.df.ufcg.edu.br/labfit/
Song X, Song S, Sun W, Mu X, Wang S, Li J, Li Y (2015) Recent changes in extreme precipitation and drought over the Songhua River Basin, China, during 1960–2013. Atmos Res 157:137–152
Stanhill G, Cohen S (2001) Global dimming: a review of the evidence for a widespread and significant reduction in global radiation with discussion of its probable causes and possible agricultural consequences. Agric Meteorol 107:255–278
Sun L, An G, Ding L, Shen BZ (2000) A climatic analysis of summer precipitation features and anomaly in Northeast China. Acta Meteorol Sin 58:70–82
Tigkas D, Vangelis H, Tsakiris G (2012) Drought and climatic change impact on streamflow in small watersheds. Sci Total Environ 440:33–41
Trajkovic S, Kolakovic S (2009) Evaluation of reference evapotranspiration equations under humid conditions. Water Resour Manag 23:3057–3067
Trenberth KE, Dai A, Van Der Schrier G, Jones PD, Barichivich J, Briffa KR, Sheffield J (2014) Global warming and changes in drought. Nat Clim Chang 4:17–22
Tsakiris G, Vangelis H (2005) Establishing a drought index incorporating evapotranspiration. Eur Water 9:3–11
Tsakiris G, Pangalou D, Vangelis H (2007) Regional drought assessment based on the Reconnaissance Drought Index (RDI). Water Resour Manag 21:821–833
Vangelis H, Tigkas D, Tsakiris G (2013) The effect of PET method on Reconnaissance Drought Index (RDI) calculation. J Arid Environ 88:130–140
Vicente-Serrano SM, Beguería S, López-Moreno JI (2010) A multiscalar drought index sensitive to global warming: the standardized precipitation evapotranspiration index. J Clim 23:1696–1718

Vicente-Serrano SM, López-Moreno JI, Beguería S, Lorenzo-Lacruz J, Azorin-Molina C, Morán-Tejeda E (2012a) Accurate computation of a streamflow drought index. J Hydrol Eng 17:318–332

Vicente-Serrano SM, Beguería S, Lorenzo-Lacruz J, Camarero JJ and others (2012b) Performance of drought indices for ecological, agricultural, and hydrological applications. Earth Interact 16:10

Wang S, Zhang Z (2011) Effects of climate change on water resources in China. Clim Res 47:77–82

Wang W, Chen X, Shi P, Van Gelder PHAJM (2008) Detecting changes in extreme precipitation and extreme streamflow in the Dongjiang River Basin in southern China. Hydrol Earth Syst Sci 12:207–221

Wang B, Zhang M, Wei J, Wang S and others (2013) Changes in extreme events of temperature and precipitation over Xinjiang, northwest China, during 1960-2009. Quat Int 298:141–151

Waseem M, Ajmal M, Kim TW (2015) Development of a new composite drought index for multivariate drought assessment. J Hydrol (Amst) 527:30–37

Willems P, Arnbjerg-Nielsen K, Olsson J, Nguyen VTV (2012) Climate change impact assessment on urban rainfall extremes and urban drainage: methods and shortcomings. Atmos Res 103:106–118

Wu S, Yin Y, Zheng D, Yang Q (2006) Moisture conditions and climate trends in China during the period 1971–2000. Int J Climatol 26:193–206

Xu XL, Huang XY, Zhang Y (2005) Statistical analyses of climate change scenarios over China in the 21st century. Adv Clim Chang Res 1:80–83

Yan D, Shi X, Yang Z, Li Y, Zhao K, Yuan Y (2013) Modified Palmer drought severity index based on distributed hydrological simulation. Math Probl Eng 2013:327374

Yan M, Deng W, Chen P (2003) Recent trends of temperature and precipitation disturbed by large-scale reclamation in the Sangjiang plain of China. Chin Geogr Sci 13: 317–321

Yang F, Lau KM (2004) Trend and variability of China precipitation in spring and summer: linkage to sea-surface temperatures. Int J Climatol 24:1625–1644

Yang JH, Jiang ZH, Wang PX, Chen YS (2008) Temporal and spatial characteristic of extreme precipitation event in China. Clim Environ Res 13:75–83

Yatagai A, Arakawa O, Kamiguchi K, Kawamoto H, Nodzu MI, Hamada A (2009) A 44-year daily gridded precipitation dataset for Asia based on a dense network of rain gauges. Sci Online Lett Atmos 5:137–140

You Q, Kang S, Aguilar E, Yan Y (2008) Changes in daily climate extremes in the eastern and central Tibetan Plateau during 1961–2005. J Geophys Res Atmos 113:D07101

Yue S, Campbell P, Pilon P (2003) Long-term water balance analysis using the complementary relationship areal evapotranspiration model. In: CSCE 16th Canadian Hydrotechnical Conference, Burlington, Ontario, p 22–24

Zargar A, Sadiq R, Naser B, Khan FI (2011) A review of drought indices. Environ Rev 19:333–349

Zhai P, Pan X (2003) Change in extreme temperature and precipitation over northern China during the second half of the 20th century. Acta Geogr Sin 58:1–10

Zhai P, Sun A, Ren F, Liu X, Gao B, Zhang Q (1999) Changes of climate extremes in China. Clim Change 42:203–218

Zhang Q, Singh VP, Sun P, Chen X, Zhang Z, Li J (2011) Precipitation and streamflow changes in China: changing patterns, causes and implications. J Hydrol (Amst) 410: 204–216

Zhang Q, Li J, Singh VP, Xu CY (2013) Copula-based spatio-temporal patterns of precipitation extremes in China. Int J Climatol 33:1140–1152

Zhang XC (2005) Spatial downscaling of global climate model output for site-specific assessment of crop production and soil erosion. Agric Meteorol 135:215–229

Zhang XC, Chen J, Garbrecht JD, Brissette FP (2012) Evaluation of a weather generator-based method for statistically downscaling non-stationary climate scenarios for impact assessment at a point scale. Trans ASABE 55: 1745–1756

Zhang Y, Xu Y, Dong W, Cao L, Sparrow M (2006) A future climate scenario of regional changes in extreme climate events over China using the PRECIS climate model. Geophys Res Lett 33:L24702

Zou XK, Zhang Q (2008) Preliminary studies on variations in droughts over China during past 50 years. J Appl Meteorol Sci 19:679–687

Editorial responsibility: Ricardo Trigo, Lisbon, Portugal

Submitted: March 7, 2017; Accepted: November 27, 2017
Proofs received from author(s): February 2, 2018